Received: 24 July 2022 | Revised: 26 December 2022 | Accepted: 18 January 2023
DOI: 10.1049/gtd2.12772

IET Generation, Transmission & Distribution
The Institution of Engineering and Technology WILEY

ORIGINAL RESEARCH

Intelligent energy management scheme-based coordinated control for reducing peak load in grid-connected photovoltaic-powered electric vehicle charging stations

Mohammad Amir[1] | Zaheeruddin[1] | Ahteshamul Haque[1] | Farhad Ilahi Bakhsh[2] | V. S. Bharath Kurukuru[1,3] | Mostafa Sedighizadeh[4]

[1]Advance Power Electronics Research Lab, Department of Electrical Engineering, Jamia Millia Islamia, New Delhi, India

[2]Department of Electrical Engineering, National Institute of Technology Srinagar, Srinagar, India

[3]Power Electronics Research Division, Silicon Austria Labs, Villach, Austria

[4]Department of Electrical Engineering, Shahid Beheshti University, Evin, Iran

Correspondence
Mostafa Sedighizadeh, Department of Electrical Engineering, Shahid Beheshti University, Evin 1983969411, Iran.
Email: m_sedighi@sbu.ac.in

Abstract

Solar-based Distributed Generation (DG) powered Electric Vehicles (EVs) charging stations are widely adopted nowadays in the power system networks. In this process, the distribution grid faces various challenges caused by intermittent solar irradiance, peak EVs load, while controlling the state of charge (SoC) of batteries during dis(charging) phenomena. In this paper, an intelligent energy management scheme (IEMS)-based coordinated control for photovoltaic (PV)-based EVs charging stations is proposed. The proposed IEMS optimizes the PV generation and grid power utilization for EV charging stations (EVCS) by analysing real-time meteorological and load demand data. The coordinated control of EMS provides power flow between PV generation, distribution grid, and EVs battery storage in a manner which results in the reduction of peak power demand by a factor of two. Further, the adaptive neuro-based fuzzy control approach includes forecasting solar-based electricity generation and EVs loads demand predictions to optimize IEMS according to the Indian power scenario. The proposed IEMS optimally utilizes the buffer batteries system for reducing the peak electricity demand with low system losses and reducing the impact of EVs charging load on distribution grid. The results are analysed using the digital simulation model and validated with real-time hardware-in-loop experimental setup.

1 | INTRODUCTION

The fast adoption of Electric Vehicle charging stations (EVCS) and extensive installation of photovoltaic (PV) plants possess huge challenges for the power flow control, especially in intermittent PV-based distribution generation (DG) penetration in the distribution grid [1]. During peak power demands, the conventional control scheme is not able to deliver the required power; also it is not capable of storing surplus solar-generated energy in the battery storage system (BSS) [2]. To deal with excess power demand and intermittent PV generation, upgradation of the distribution network may not be cost-effective. Thus, it can be said that such a large capacity battery will reduce the impact on the grid but increase the overall cost of the system. In order to achieve optimal scheduling of EV charging and solar PV energy according to the current distribution network, the better utilization of solar-powered EVCS with a backup BSS is an effective way to maintain the charging load, improve the distribution grid stability, and maintain an uninterrupted power flow for EVCS [3]. Presently, the EVs charging/discharging coordinated control is accomplished with different levels of EVCS at different stages, namely AC (level 1/2/higher) [4], DC fast (level 1/2/3) [5], and DC ultra-charging [6]. The AC level 1 (1.4−2.4 kW) is used in homes/offices, and AC level 2 (7.7−25.6 kW) onboard charging is deployed in private or public outlets. Fast DC (up to 240 kW) offboard charging is mainly used in commercial, conventional filling station, and office areas [7]. In the literature [8], only a small number of PV-based EVCS with BSS devices have been modelled, and mostly these stations instantly replenish the batteries after each charge cycle. For the day ahead energy management schemes (EMS), only few research has accounted for PV power prediction with EV charging load forecasting. Most of the PV-based EVCS with buffers BSS have not been depicted and also were not incorporated with accurate PV generation prediction and EV load demand estimation into their optimal EMS [9]. At present, PV-based EVCS with buffer BSS operate with an always full-recharged battery or are immediately recharged to a fixed state of charge (SoC) from PV power and/or the local grid after each charging event. The PV-powered EVCS with buffer storage decreases the local grid peak power demand. But uncoordinated system with inconsistency in DGs forecasts may lead to unscheduled charge of the buffer storage, further EV charging load consumes more power without the PV power availability.

The growing solar PV-based renewable energy generation has decreased the burden on the modern grid system and offers a consistent and reliable power supply to the EVs load [10]. On the other hand, the solar-powered PV generations introduced an option for the electricity consumers and power utilities to operate in standalone (SA) and/or grid-connected (GC) operational modes [11]. The EVs load with deregulated power system delivers the complex operational situations for the distribution companies (DISCOs), that is, during EVs load synchronization with the grid [12]. Whenever the PV system is operating in the GC mode, there should be a necessity for voltage as well as frequency synchronization [13, 14]. In case of an unintentional grid fault, the DGs separate from the utility grid and the backup storage system maintains the additional EVs charging load. Moreover, when the load demand surpasses the PV generation capacity then the grid feeds excess electricity to the EVs load during GC mode and at the same time need to be grid operation is in a constant mode without any interruption. In another study, the adaptive neuro-fuzzy interface system (ANFIS) controller produces the reference values based on the grid voltage (v_g) and the grid current (i_g) [15]. While in the SA mode, the ANFIS controller produces the reference values internally as per the PV data and EV charging load demand. The various traditional charging strategies adhere to the charging interfaces with novel strategies available for minimizing the impact of EVCS on the distribution grid being discussed [16]. The investigation of research gap for different control approaches in comparison with the existing literature [17–23] is presented in Table 1.

The investigation of the control strategies for PV-powered EVCS control in terms of similarities and differences is as follows: In [18], the fuzzy inference system (FIS) was designed for the grid synchronization technique in the GC and SA modes using the droop controller; however, in our proposed work, an unintentional islanding detection and its classification in distributed sources is an add-on feature as compared with [18]. Further in [23], a deep neural network (DNN)-based short-term forecast model of EVs load demand was designed. But it is suitable for only grid to vehicle (G2V) operation. Reducing the power demand burden on the local grid during EV charging events is a major similarity for different control approaches. The proposed intelligent energy management scheme (IEMS) feeds the PV power to the EVs charging load, and at the same time surplus electricity is supplied to the utility grid. Data overfitting is a major problem to check the errors in the training process [24]. The data sets from one charging station are contingent on EVs dis(charging) behaviours, whereas more data can be taken from multiple charging systems in order to deliver accurate charging load projections and avoid overfitting issues.

This study estimates the optimal SoC of the workplace for the next months, which is based on a daily historical EVs charging data set using a linear fit analysis to derive the charging patterns. The major difference with existing systems [25] is that the proposed adaptive control approach does not need information on EV driving patterns (departure time and arrival time) to achieve the optimal IEMS. Thus, to understand the superiority of the proposed adaptive neuro-fuzzy-based control technique based on research gap with the existing control strategies [17--23] is presented. Also, the impact of EVCS on the distributed grid is higher in conventional control strategies as referred to in existing literature [26, 27]. The grid operators use classical-based control techniques in operations rather than the intelligent control techniques because the classical control techniques have the capability to utilize the closed-loop systems in terms of open-loop systems, on the other hand, which are established or easy to design. Besides, with all features, classical control techniques are lacking with respect to coordinated control. So, our proposed coordinated control scheme is superior to classical techniques, because it minimizes the impacts of EVCS on the distributed grid. The proposed study provides flexibility for the DG-based EVs aggregator system and further, it will be beneficial for generating companies (GENCOs) in planning by forecasting their daily EV charging demand with respect to local generation activities. Thus, the motivation of this study is to design and deploy an intelligent adaptive controller to reduce the adverse impacts of EVCSs on the local grid and maintains the SoC level of BSS with effective utilization of PV-based DGs. The following are the key contributions:

- Investigates the supervisory of the proposed adaptive neuro-fuzzy control strategy for two different case studies (with or without buffer storage system) under flexible weather conditions to project the cumulative grid electricity response as per past solar PV generation and the EVs charging load data accordingly.
- The novel contribution of the proposed intelligent coordinated control system is automatically switching to desired operational modes (GC or SA).
- Examines the SoC of a storage system and how it varies with respect to optimal range based on the historical real-time weather data under the EVs charging events.
- Designs an IEMS for solar-powered EVCS by employing DG power forecasting with EVs charging demand data for cumulative electricity management.
- Analysis of various EVs dis(charging) operations using hardware-in-loop (HIL) emulator in order to verify and control peak power requests from dynamic EVs charging load.
- Operates the system in different scenarios to maintain the EVCS load based on the effective utilization of battery storage using the coordinated control scheme.

TABLE 1 Comparative literature review of different control strategies for research gap

Control strategies	Key findings/potential applications	Configuration/ operation mode	Research gap	Ref.
Grey theory optimization and neural network (NN)	Analyzed effects of multiple environmental factors for PV and EVs charging load prediction	Uncoordinated control, GC mode, G2V operation	Elimination of cumulative errors for non-linear load sequence	[17]
Fuzzy inference system	Grid synchronization technique using droop control	GC and SA mode	Unintentional islanding detection and classification in distributed sources	[18]
Discrete-based Markov decision control (MDC)	Projected the EVCS load, PV power, and optimized BSS unit with SoC range (0.3–1)	G2V GC/SA mode	Varying solar irradiance and local load only for individual day	[19]
Autoregressive integrated moving average (ARIMA)	The energy management approach for PV electricity forecast to charge the EVs aggregator	Uncoordinated control, V2G/G2V operation	Optimization of power flows between the PV system, local grid, and a BSS to decrease the EVs charging cost	[20]
Mixed integer linear programming (MILP)	PV power and EVs arrival forecast at EVCS for total profit maximization	Uncoordinated control, G2V operation, GC mode	Profile maximizes without any optimization technique and hardware validation	[21]
Stochastic programming	A case analyzed for day-ahead price forecast at a parking lot with 50 EVs	Coordinated control, V2G operation	Consideration of several possible EVs dis(charging) patterns	[22]
Deep Neural Networks (DNN)	Short-term forecast of EVs load demand	Dynamic control, G2V operation	Adverse impacts of peak EVs charging load on distribution grid	[23]

Abbreviation: G2V, grid to vehicle.

- Further, validates the intelligent EMS with buffer storage system under the peak power demand of EVs dis(charging) load at different instants of time.

The innovation in this research with respect to the existing literature is to design IEMS along with the buffer storage control scheme, which is capable of reducing the peak EVCS load demand on the main grid. Further, the major innovation in the optimal transition control strategy is disconnecting the DG system from the local grid under different scenarios (grid failure or off-peak conditions) and reconnecting the DG system again without the BSS. The proposed strategy overcomes the impacts due to the non-linearity present in the PV-based DG system and maintains the flexible EVs charging demand with the regulation of dis(charging) for a BSS. The significance of the proposed IEMS approach lies in maximizing the PV-based DG for EVs charging and reducing its impact on the grid, especially during peak loading scenarios. One of the major challenges is optimal power flow control between the utility and EV charging load to design an intelligent energy management scheme (IEMS) framework. It can be significantly overcome by designing an IEMS for controlling the power flow between the local grid and the EVs load. However, in our proposed system the power flow control is bidirectional, that is, both G2V and vehicle-to-grid (V2G). Also, the advantage of our proposed adaptive controller is to enhance the real-time charging control in solar-powered EVCS by V2G ancillary services.

The remaining sections of the research are organized as follows: Section 2 describes the design of the proposed intelligent EMS and details the requirements for optimizing an IEMS. Section 3 discusses the coordinated control strategies and development of the intelligent controller, while Section 4 presents the digital simulation analysis of different case studies and its validation using the real-time HIL experimental setup given in Section 5. To understand the action of the proposed control approach, the SoC levels of different scenarios are plotted under possible intermittent PV generation variations. Further, the novelty of the proposed control approach is summarized in the Result section. In the Results section, the comparison of the proposed control approach with the conventional techniques is discussed. Finally, Section 6 concludes the research paper.

2 | DESIGN AND OPTIMIZATION OF PROPOSED EMS

In this section, the design and optimization of the proposed IEMS is presented. For this, the present study demonstrates the utilization of real-time metrological data and actual EVs charging load statistics in an optimal EMS. To maximize solar energy usage, reduce peak power consumption, and sudden spikes on the distribution grid during EV charging a coordinated control system is required [28]. On the basis of the extracted weather real data sets, PV electricity is forecasted as per the actual PV electricity generated data. More accurate short-term weather information in PV electricity forecasting models could increase the accuracy of the demand response estimation [29, 30]. Here, the design of BSS optimization aims to predict actual EVs load statistics into the EMS with a buffer storage system in order to maximize the utilization of PV-based electricity and minimize the fluctuation of the voltage profile on the distribution

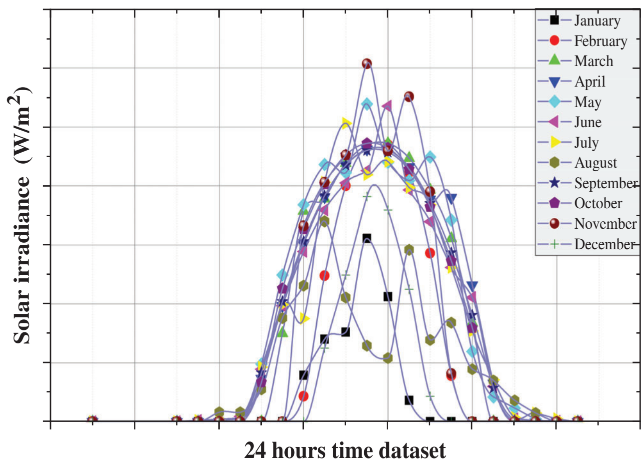

FIGURE 1 Yearly solar insolation data.

grid. By using the ANFIS controller, weather forecasts for EV charging and generated PV power are used to address uncertainties associated with EVCS usage including dynamic dis(charging).

2.1 | Meteorological data and PV electricity forecasting

Accurate forecasting is essential in order to efficiently utilize and manage solar-based electricity. The PV energy generated is directly dependent on the amount of incoming solar insolation, the panel temperature, and the panel V to I characteristics. Also, there is spatial and temporal variability in solar insolation [31]. During a clear sky, solar insolation on the PV panel is measured by multiplying the individual day, and hour of that day by the cosine function of the angle (the angle in between normal to the Sun's direction and tilt PV panel). The amount of solar energy that reaches the solar panel changes according to the state of the sky. Numerous complex models have been established to evaluate the actual PV generation to manage grid power [32]. Here, the metrological information is gathered from the open-access WeatherMap website [33].

Figure 1 shows the yearly solar irradiance data in a CSV format, which is streamed in a plotting tool [34]. Here, the cloud cover is calculated to forecast the solar insolation for Delhi, India region [35]. In the case of an EVCS equipped with limited BSS, accurate solar power forecasting can be beneficial to control the grid power [36]. The calculation of PV-based electricity is based on the most common indicator of the per cent of cloud cover and the state of the sky. In order to simplify the electricity forecasting model, cloud cover is referred to as a percentage reduction in solar insulation in comparison with a clear sky. The projected solar electricity generation is calculated by the addition of measured solar insolation by multiplying the PV panel area by the solar panel efficiency over the random time period, which is mathematically expressed in Equation (1).

$$E_{PV}^{F} = A \times \eta \int (1 - C_c) . I\,(d, t)\, dt \tag{1}$$

In Equation (1), E_{PV}^{F} is forecasted PV electricity (Wh/m^2) on daily basis, A is the PV panel area in m^2, η is panel efficiency, C_c is cloud cover, and $I(d, t)$ is the solar insolation (in W/m^2) collected by the solar panel on a random day. Here, $I(d, t)$ is simulated as a 2D array, which is indexed by a random day of the year.

2.2 | EVs charging load estimation

The optimal performance of PV-powered EVCS with buffered BSS is controlled by forecasting of charging load. The forecasting of EV charging demand is vital for intelligent energy management. For optimal control of grid power, medium- and long-term EV charging load estimation schemes have been demonstrated in [37]. Most approaches utilize statistical methods, which are based on past data sets including EV charging load and meteorological data variation with respect to time. However, the charging rate for EVs may greatly vary and depends on vehicle driving patterns, charging routine, and other time-dependent variables such as the day of the week including the holiday [38]. The conventional EVs load forecasting techniques may not be feasible for projecting the EV dis(charging) load with respect to the power demand. The charging power of vehicles cannot be accurately predicted at a specific time, but the average energy consumption of the number of EVs at a commercial charging station can be predicted based on the charging routine. Thus, the estimation of EVs dis(charging) and average energy demand at a particular time can be projected using historical EVs charge pattern data sets. To modify the existing forecasts model in the direction of avoiding the requirement of inaccessible weather data information, a coordinate is designed that controls the EVs charging load parameters over 3 months' period from the historical charging dataset. The average EV charging load demand for a particular instant is forecasted using the same day of an individual week, which collects past EV charging load data for the same day of the week as the forecast period. Here, the least-squares approach is used which includes the linear fit method of past vehicles dis(charging) load data set to forecast the EV charging demand for a specific day.

The proposed least-squares approach is employed to fit the past EVs charging data sets for power consumption demand to a straight line as a generalized form in Equation (2).

$$E_{EV}^{F} = s.n_w + b \tag{2}$$

Here, E_{EV}^{F} is forecasted vehicle charging load in $\frac{\text{kWh}}{\text{day}}$ for the n number of days. The data point for a random day of an individual week is represented by an integer n_w and b is representing the intercept in the fitted model for a week ($n_w = 0$) and s is representing slope. The values of s and b represent the optimal fit of past EV charging consumption data for each day of a week over the past 3 months' data. When evaluating the optimal fit, $n = 7$ is set for each day of the upcoming week to determine the forecasted EV demand at the workplace or charging station.

2.3 | Optimization of battery storage SoC

In this section, the key objective is to optimize the SoC of the buffer battery storage and eliminate the unregulated charging under the variation of dynamic EVs charging load. In order to achieve this, the corresponding control logic associated with EV charging load variation is calculated using a supervised algorithm. Initially, the input signals to the HIL are sampled and used with the model-sim programming. As all the operation is carried out with python simulation aspects and the HIL interface, the graphs are plotted as a time series representation based on the data accumulated while conducting the experiments. Hence, all the results are visualized using the simulation tools only. Most of the vehicle charging at workplaces occurs during the morning hours and during this time PV power generation is low. So, BSS must be sufficiently charged to fulfil the estimated charging load demand during peak hours [39]. Equation (3) gives the desired SoC at the start of the day.

$$\Delta E_{BSS}^{F} = E_{EV}^{F} - E_{PV}^{F}, \quad \left(SoC_{max} \geq SoC_{n}^{F} \geq SoC_{min} + \frac{kE_{EV}^{F}}{E_{BSS}} \right) \tag{3}$$

where $SoC_n^F = SoC_{mean} + \frac{k\Delta E_{BSS}^F}{E_{BSS}}$

When the battery SoC level is less than the estimated SoC, then it needs to be maintained the EVs charging demand and the BSS must be recharged by the distribution grid throughout the off-peak period. For this reason, the battery storage SoC at the start of a day needs to be kept at the desired level, which depends on the variation between the forecasted PV generated power with respect to the estimated EVs load charging requirements for an individual day. Thus, SoC_n^F is obtained by Equation (3) at the start of the day. Here, the SoC_n^F means forecasted desired SoC level at the start of the nth day. This is equal to the sum of SoC_{mean} (mean SoC level in % at the start of the day without overnight vehicles charging) and the ratio of $k\Delta E_{BSS}^F$ to the E_{BSS}. Here, $\Delta E_{BSS}^F = E_{EV}^F - E_{PV}^F$ is forecasted electricity of BSS, which shows the deficit electricity and surplus electricity ($+ve$ means deploying and $-ve$ means charging). E_{BSS}^F is representing the total BSS capacity in kWh. But, K is an account for the correction factor for losses in BSS and conversion (it is assumed $k > 1$). Here, E_{PV}^F is forecasted PV electricity in kWh for the next day (referred from Equation (1)) and E_{EV}^F is forecasted EV charging load demand in kWh for the next day (referred from Equation (2)). The SoC_n^F lies in between SoC_{max} (maximum SoC level in %) and the sum of SoC_{min} (minimum SoC level in %) with the ratio of kE_{EV}^F is forecasted vehicle charging load in $\frac{\text{kWh}}{\text{day}}$, for the next day (referred from Equation (2)) and E_{BSS}.

3 | COORDINATED CONTROL STRATEGY

A dynamic control strategy has been designed for utilizing maximum generated power for reducing monthly peak load consumption [40]. This dynamic control approach is only limited to domestic EVs charging load and it is manually controlled by distribution system operators (DSO). Further, a conventional transactive-based energy management strategy for PV-based less number of EVs integrated parking lots GC system has been demonstrated in [41], and a stand-alone (SA) charging station integrated with a mini-grid for rural applications depending on the availability of local electricity has been demonstrated in [42]. Here, the coordinated control system operation is automatically switched to the desired mode (GC/SA). The EVs are plugged into the EVCS in the GC mode and BSS is charged by the PV energy if it is available. In the SA operation mode, the PV power is utilized to charge the EVs. If more energy is required, it can be provided by the utility grid or/and by the BSS. Solar power is stored in the BSS if no EV is plugged in, and surplus solar power is fed to the local grid (if the BSS is fully charged). The battery SoC can be brought up to an optimal level by grid power during off-peak hours (if the BSS charge level is low). Thus, as per the estimated PV generation and estimation of EV load charging demand, the desired battery SoC can be evaluated.

In [43], a BSS functioned as an uninterrupted energy supply system, where the storage remains charged as per the schedule, which acts as only an emergency backup supply system. The benefit of operating the proposed system in GC operational mode is that during the condition of EVs load demand exceeds the generated capacity of DG system, so the local grid provides surplus electricity to fulfil the EVs load demand and there will be power maintained without any interruption. So, the proposed coordinated control strategy has the novelty that it differs from the previously developed systems based on various control aspects and response time. In the case of without consideration of the off-peak time (if the voltage of BSS reaches the lower limit), the distributed energy resources (DERs) system charges the BSS to the desired voltage limit from the solar-based power generation and/or by the distribution grid. Here, the proposed system is used as an ANFIS controller interface with supervisory control in order to bi-directionally communicate with the voltage source inverter (VSI) over the MOD/controller area network bus. From Figure 2, the coordinated system controls the PV-based DGs power and monitors the BSS status, EVs charging load, and grid availability/unavailability status in order to control the active power flow between other power system components based on the mode of operation [44]. To optimize the storage system, a coordinated control strategy must require information on SoC status, BSS flexible capacity, and

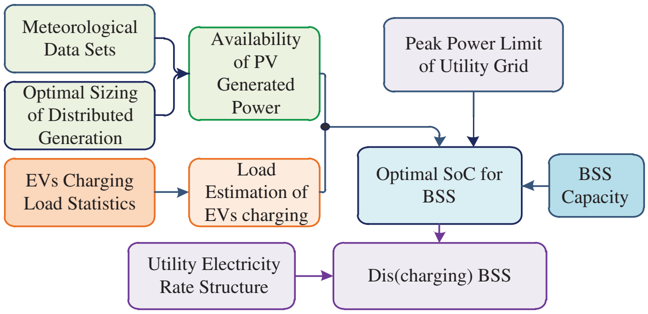

FIGURE 2 Coordinated control of battery storage system (BSS) with optimal state of charge (SoC).

dis(charging) rate with respect to load. The key advantage of coordinated control for the EVCS owner is through the time of use with specified electricity rate structures in respective of peak power limit and tariffs. The utility electricity rate structure is considered to reduce the electricity cost during dis(charging) the BSS from/to the utility grid if required under on/off-peak hours scenarios. The control approach includes forecasting of solar-based electricity generation and EVs loads demand predictions to optimize IEMS according to the Indian power scenario, for it the utilizing electricity rate structure data is taken from the National Renewable Energy Laboratory database [35].

The supervisory control utilizes the variable weather condition data sets from a load-generation prediction website to estimate the solar generation and forecasts the estimated vehicle charging load as per the past stored dis(charging) pattern of the EVCS [33]. According to the operational mode, the generated DGs power can feed to the EVs charging load, and surplus electricity is supplied to the utility grid. If disturbances occur, then the hybrid DGs will be decoupled from the main grid and the buffer storage system will maintain the additional EVCS load. To optimize the SoC of BSS in the EVCS during the off-peak duration, the optimization approach is employed for the estimation of solar generation and EVs charging load is referred to in Figure 2. Figure 2 highlights the features of a coordinated system through supervisory control for bidirectional communication with VSI over MODBUS and the EMS for storage over CANBUS [45]. The intelligent coordinated controller uses the past data from the PV panels to estimate the available DG power and estimates the required EVs charging loads based on previous charging patterns and weather conditions. To estimate the possible impact of DG and EVs charging load on the local grid network, the simulation study has been performed using a buffer BSS for EVs charging by DG powered (P_{DG}). The P_{DG} and EVs charging demand based on the real operating conditions of the charging pattern under different scenarios are represented by the flowchart as depicted in Figure 2.

3.1 | Power flow and transition control scheme

The aim of transition control is to obtain fast response in order to operate the DG system in both GC and SA operation modes.

TABLE 2 Operational modes of the PV-powered EV charging load equipped with BSS

Mode of operation	Power flow
Mode 1: GC operational mode	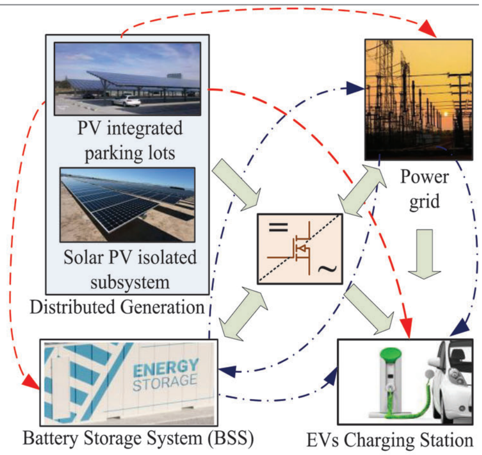
Mode 2: SA operational mode	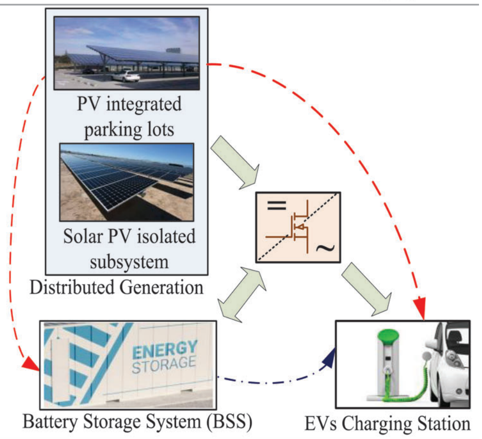

Further, the simulation study performs for the quick transition between GC operation mode, which is based on the off-peak periods scenario and SA operation mode, which is based on the on-peak periods. Thus, optimal transition control is achieved by developing a supervised IEMS. In the distribution system, BSS never feeds energy to the utility grid due to higher charging load requirements and lower generated power availability. In the GC operational mode, the grid power (P_G) is not available at all times [46]. In addition to charging EVs, the distribution system supplies non-linear loads that cannot be directly supplied by the grid [47]. Consequently, the PV will supply energy to the EV charger (if it is available), while the battery may provide energy (if needed). The BSS will store the remaining PV energy if surplus energy is available. By using the buffer BSS, the distribution system can feed reliable as well as constant energy from intermittent solar PV to satisfy the charging load.

As shown in Table 2, the dis(charging) of BSS during the off-peak durations depends upon the PV-based DG and the EV charging load. Here, mode 1 (GC) and mode 2 (SA) illustrate that the proposed system operates under uninterruptible power flow mode. The BSS in mode 2 is always fully charged and serves as a backup power supply source system. At the lower limit of BSS voltage, the intelligent coordinated system charges the BSS to the upper voltage limit with high capacity from either the solar-based DG power and/or the power grid without taking into account the off-peak durations. An intelligent controller monitors the status of PV electricity status, BSS status, EVs dis(charging) pattern, and local grid status in order to control the power flow between other system components [48]. The proposed control approach aims to reduce the P_G demand, maximization of distributed generations (DGs), optimal SoC of BSS, and maintaining the EV_S charging load.

As per the availability of P_G, the EVCS operates in two modes (mode 1 is grid-tied and mode 2 is stand-alone). In mode 1, the EVs charge from DG, BSS, and grid. However, in case of a grid fault or power outage, the proposed coordinated system will be isolated from the grid, and it will automatically switch to mode 2. In mode 1, during plugging of the EVs into the charger, if P_{DG} is available then it is used to control the EVCS. Further, if more power is needed to charge the EVs, then the remaining power is fed by the BSS/grid. If there is no plugging of EVs, then P_{DG} is stored in the BSS and if BSS is fully charged, then surplus P_{DG} fed into the grid. In case of off-peak hours, if BSS is insufficiently charged, then P_G can be utilized to fulfil the SoC level of BSS up to the desired level. Once the BSS is charged up to the desired level even though the desired power cannot be fed from BSS to the grid, due to the high-level requirements of EVs charging load. In mode 2, the P_G is not available. The proposed system can feed power to additional critical loads economically and reliably. If DGs are available, then the DGs will feed power to the EVs charging load. At this time, if sudden EVs charging demand increases then that demand will be fulfilled by the BSS. If surplus power is available, then the remaining P_{DG} is stored in BSS. Hence, the proposed coordinated system is working as a constant reliable power source.

In Figure 3, the flowchart of control logic is for both GC and SA modes of operation. Here, P_{EVSE} is the power of the EV supply equipment. When $P_{DG} < 0$, depending upon the mode of operation of the EVs charging station, that is, GC (mode 1) or SA (mode 2) operation mode, the charging demand of the EVs is fulfilled either by the grid or by the buffer battery storage based on its optimum SoC levels. From Figure 3, P_G is grid power, P_{DG} is the output power of DG, P_{EV} is the power required by the electric vehicle supply equipment (EVSE), P_{BSS} is BSS power (where ($P_{BSS} > 0$) means BSS discharging). Here, P_{DG} ($-ve$) means: DG charges the BSS. If the $P_{EVSE} > 0$ then the supervised control will check for the SoC requirement either to charge the battery or to reset the battery power to zero and start checking for the transition. The default value of the targeted SoC is taken as $SoC_{tar} \geq 0.80$, P_{CMD} is the power command during off-peak hours for charging of BSS (default value = 0). The SoC_{tar} and P_{CMD} can be controlled by a supervisory commuter. The P_{CMD} depends on the availability of the DG power, the SoC of BSS, the EVs charging load, and the status of the charging system, type of system operating modes (either GC or SA). This maintains the power flow (during on/off-peak hours) for charging the BSS from the grid using the proposed IEMS.

3.2 | ANFIS control strategy

The ANFIS incorporates the optimal features of artificial neural network systems (ANNs) with a FIS to realize the power flow information based on the training dataset. The proposed FIS guides a rules base, attributes of input/output, membership functions (MFs) of input/output, and decision variables related to desired single-value output. The ANFIS model is designed by the FIS whose MFs are customized either through an algorithm (least-square type or backpropagation) for variable input/output data sets [49, 50]. The architecture of the proposed ANFIS is depicted in Figure 4.

The ANFIS architecture comprises five distinct layers with number of inputs as error (e_1) and change in error (de_1) that are associated with layer 1. The output of layer 5 is f, which provides the summation of all incoming signals associated with the adaptive node. In Figure 4, the adaptive nodes are referred to by a square and a fixed node is referred to by a circle. All layers have a distinct function that is suitable for obtaining input/output data sets. Some layers have a similar number of nodes, with analogous functions. The adaptive network is usually trained through a hybrid-based learning algorithm grouping of least-squares type (hybrid learning algorithm) and backpropagation type (gradient-descent (GD) algorithm). Thus, it allows the FIS to learn by the data set and is intended at corresponding the proposed ANFIS output with the trained data set [51]. To get the desired outputs and the error rates (d/de) execute the proposed system for all iterations. Further, the training dataset is exported to FIS controller for test output response. The rule base can be formulated by the function of each layer:

Rule 1: If e_1 *is* X_1 *and* de_1 *is* Y_1, *then*

$$f_1 = p_1.e_1 + q_1.de_1 + r_1 \tag{4}$$

Rule 2: If e_1 X_2 de_1 Y_2, *then*

$$f_2 = p_2.e_1 + q_2.de_1 + r_2 \tag{5}$$

Rule n: If e_1 X_n de_1 Y_n, *then*

$$f_n = p_n.e_1 + q_n.de_1 + r_n \tag{6}$$

The crisp inputs to the nodes are e_1 and de_1. Here, the X_1, Y_1, X_2, Y_2, …, X_i, Y_j, are the proposed fuzzy sets, and output function (f) varies with respect to the related weight function (w_n). The node in the $i$thposition of the nth layer is represented by $O_{n,i}$ and the role of each node in the similar layer is the identical function that can be depicted as follows:

Layer 1 is an adaptive node, where the input layer and each node i have a node function Equation (7). $O_{n,i}$ is the MFs of X_i, which specifies the degree of error and accordingly provides the

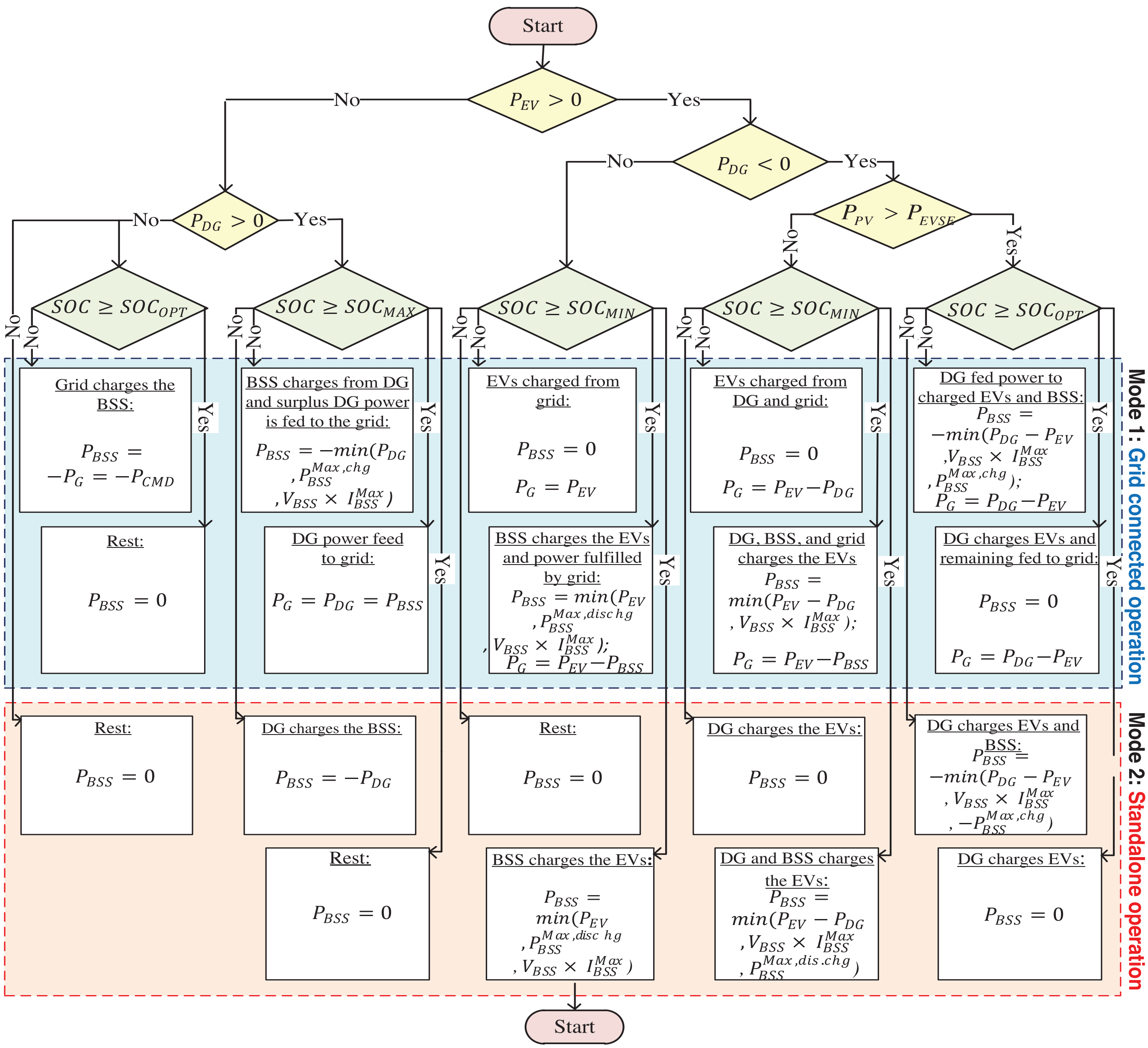

FIGURE 3 Supervised control flowchart for two modes of operation such as GC (mode 1) and SA (mode 2), respectively. GC, grid-connected; SA, standalone.

value of proposed quantifier (X_i). In this paper, the Gaussian bell-shaped input MF is chosen as MFs ≥ 1 as referred to in Equation (8).

$$O_{1,i} = \mu.X_i\left(e\right), \text{for } i = 1, 2, 3, \ldots, n \tag{7}$$

$$\mu.X_i\left(e\right) = \frac{1}{1 + \left[\left(\frac{x-\gamma_i}{\alpha_i}\right)^2\right]^{\beta_i}} \tag{8}$$

Here, α_i and β_i (positive value) varying the curve's width accordingly, and while γ_i represents the centre of the curve, which is also called as 'antecedent parameters'.

From Equation (9) in layer-2 the w_i denotes the firing strength of the related rule base, the node function multiplied by the input signals to get the output response. Each node is fixed, which is marked by a 'P' within a circle as shown in Figure 4.

$$w_n = O_{2,i} = \left[\mu.X_i\left(e\right)\right]\times\left[\mu.Y_i.\left(de_1\right)\right], i = 1, 2, 3, \ldots, n \tag{9}$$

Layer 3 is almost the same as the previous layer 2, each node in this layer 3 is also fixed that is marked by a }N′ within a circle. The normalization of w_n with respect to node function is evaluated by taking the ratio of the related node and the ith node. Thus, the summation of the overall w_n to all rules base is depicted in Equation (10).

$$\bar{w}_n = O_{3,i} = \frac{w_n}{w_1 + w_2}, \textit{for } i = 1, 2, 3, \ldots, n \tag{10}$$

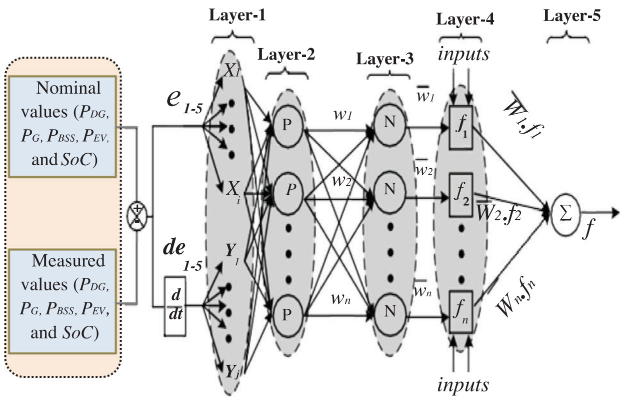

FIGURE 4 Modified architecture of ANFIS for the reduction in grid power (P_G) demand and maximize the P_{DG} for optimizing EVs charging (P_{EV}) to optimize the SoC of BSS capacity. ANFIS, adaptive neuro-fuzzy interface system; BSS, battery storage system; EV, electric vehicle.

In layer 4, the ANFIS employs the least-squares technique to identify the best-suited desired parameters. In layer 4, each node functions as an adaptive node. Equation (11) refers to the parameter (p_i, q_i, and r_i) of linear functions in the Sugeno type model. Equation (11) is associated with the consequent parameter's node.

$$O_{4,i} = \bar{w}_n \times f_n = \bar{w}_n \times \left(p_1.e_1 + q_1.de_1 + r_1\right) \tag{11}$$

Layer 5 is having a single or fixed node which provides the best-suited output response followed by a summation of all incoming signals (referred to in Equation (12)).

$$O_{5,i} = \sum_n (\bar{w}_n.f_n) = \frac{\sum_{n=1}(w_n.f)}{\sum_{n=1}(w_n)} \tag{12}$$

The MF parameters of FIS can be adjusted by the GD method, which is also known as the back-propagation method. The proposed ANFIS is trained by adaptive control to match the training dataset with the desired output response. During the forward pass, the least-squares scheme is employed, once the desired parameters are obtained then the backward pass initiates to get desired parameters based on the best-fit dataset. For training analysis, the adaptive neuro-fuzzy simulation is performed by data collection and normalization. Further, the remaining data sets are referred to for testing purposes. Then, to validate the proposed ANFIS model the dataset is classified for checking the optimal values. During validation, the main concerns are over-fitting during the training and checking of errors [24]. Preferably, the errors must be reduced during the training period. If an error is not decreasing, then it signifies over-fitting. On the other hand, if the error rises in the initial iteration before the system is trained, then FIS must be re-trained, because these MFs may not be able to get the optimal selection for modelling of the remaining dataset. Thus, one must use either other MFs or increments in the dataset. These errors are evaluated by the

TABLE 3 Proposed parameters for modelling criterion of ANFIS controller

ANFIS parameters	Value
Number of inputs	10
Membership function	Gaussian bell-shaped
Number of MFs	Varying between 5 and 7
Type of learning algorithm	Hybrid
Number of iterations	500–1000
Proposed fuzzy system	Sugeno
Output type	Linear/constant
Step size	Initial size 1.1, decreased to 0.90
Nodes	110
Fuzzy rules	25–49

root mean square error (E_{RMS}) analysis:

$$E_{RMS} = \sqrt{\frac{\sum_{t=1}^{n}\left(\hat{V}_t - V_t\right)^2}{n}} \tag{13}$$

In Equation (13), the $\hat{V}_t$ are estimated values and V_t are the desired target values for time (t), where the number of samples is n. The design of the proposed ANFIS controller and its optimal parameters are depicted in Table 3.

To detect the real-time control action of the ANFIS controller in the transition period, a real-time HIL simulation model is developed. The real-time results of the proposed controller show the speedy grid conditioning monitoring under 12 ms.

3.3 | System configuration

The proposed framework of the coordinated control system is to be simulated, which is depicted in Figure 5. Two PV systems with different power ratings are designed to represent the PV-integrated parking lots and an isolated PV substation. The combined power output of these plants is fed through a 50-kW bi-directional DC–DC converter unit (these converters operate with the charging station requirement in the parking lot along with the BSS) and DC–AC converter unit (this converter operates the PV systems along with the charging stations and BSS in the GC mode). The bi-directional functionality helps in providing grid-feeding opportunities to the PV, EVs, and BSS. It operates the converter in rectifier mode to feed the EV, BSS, and local loads during low PV or no PV scenarios. Moreover, the framework adopts the ANFIS-based EMS to achieve coordinated control between the sources, loads, and grid to reduce peak loading on the grid.

The proposed grid system is integrated with DGs (a 5-kW PV subsystem integrated with a parking lot and a 5-kW isolated solar subsystem), three EVs charger units (3.3, 6.6, 3.3 kW), a 70-kWh BSS size, and a 20-kW load response bi-directional converter. The proposed subsystem parameters are shown in Table 4. (ANFIS) controller produces the reference

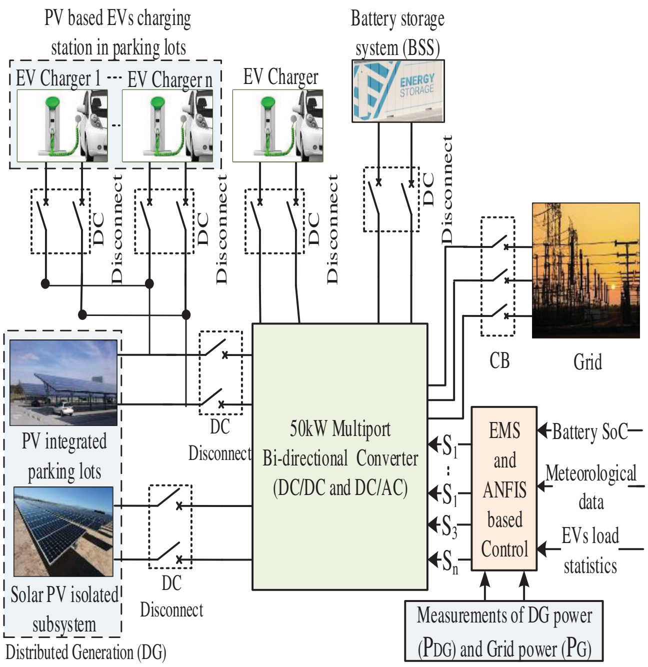

FIGURE 5 A framework of the proposed system with BSS and PV-based distributed generations for GC/SA mode. PV, photovoltaic.

TABLE 4 Simulation parameters of EV charging station

Subsystem parameters	Rating
Distributed generation (DG) system	A 5 kW solar PV panel integrated with a parking lot and a 5 kW isolated solar plant (250–600 V_{DC})
Multiport bi-directional converter (DC/DC and DC/AC)	20 kW
Type and number of EVs charger	PHEV and three chargers
Charger (rating)	3.3, 6.6, 3.3 kW with different charging times
BSS capacity	$275 - 400\frac{V_{DC}}{70}$ kW (lithium iron phosphate battery)
Utility grid	415 V

values based on the grid voltage (v_g) and the grid current (i_g) [15]. In the SA/GC mode, the ANFIS controller produces the reference values internally as per the EV charging load demand.

Initially, the charging station feeds continuous power without optimization of BSS to receive data on EVs load which is employed for predicting the EVs charging load. Further, the optimization of the BSS function is initiated in order to maintain the SoC level of BSS (as projected by PV generation and associated load). During the off-peak hours, (9 pm–7 am), BSS is re-charged to the fixed optimized value of SoC which is equal to 0.8. In the simulation, the dataset of P_{DG}, P_{BSS}, SoC, P_G, and EVs load are collected at every minute. The proposed EVCS is continuously operating either in GC or in SA mode for maintaining the EVs load level. To validate the ANFIS control approach, the data collection for system operation is a primary task.

4 | SIMULATION RESULTS AND SYSTEM OPERATION

To realize the impacts of the DG system and EVs on the local grid, the solar-powered EVCS is simulated. The simulation study of optimal transition control is presented for scenario 1 (without buffer BSS) and scenario 2 (with buffer BSS) in order to validate the response of control action of coordinated DG system in both GC and SA operation modes. Further, the simulation study identifies effective operation and quick transition between GC operation mode during the scenario of off-peak periods and SA operation mode during the on-peak periods.

4.1 | Scenario 1: DG-powered EVCS without buffer BSS

In this scenario, the energy management of a PV-powered charging system fulfils the EVs charging demand with effective utilization of solar irradiance, especially during the daytime period. In this scenario, there must be a requirement for intelligent EMS, which decreases the local grid peak power demand for EV dis(charging) load at different instants of time. In a typical scenario to be simulated, the three onboard EV chargers having maximum charge rates of 3.3 and 6.6 kW are used for simulation analysis. Since, if the EVs batteries are approximately less than half their discharge rate, then the EVs' owners charge their EVs batteries. In this simulation, the total EVs charging load is taken as 13.2 kW (3.3, 6.6, and 3.3 kW) which operates in the different instants of time, respectively. The BSS capacity is 70 kWh with their operational SoC within the range of 0.4 to 1.

In Figure 6, the different scenarios of solar-based DG power (with or without PV output power) have been taken for individual days to validate the proposed system. The output power of PV systems throughout the day is characterized by the sin wave curve from morning 9 am to evening 6 pm with an average peak power of 6.4 kW for Day 1, 2, 4, 5, and there is no PV power on Day 3. The input characteristics of the proposed charging system are kept with similar considerations as in practical operating consequences. In this paper, two different cases of battery storage optimization have been simulated for DGs-powered EVs with backup BSS.

Case 1 is to recharge the BSS instantly to the desired level within 1 to 2 h after every EV charging cycle. In this simulation, a fixed target of SoC is 0.8 employed with a charging power of 10 kW.

And another case, that is, Case 2 is employed during the off-peak hours to optimally charge the BSS. The optimal value of

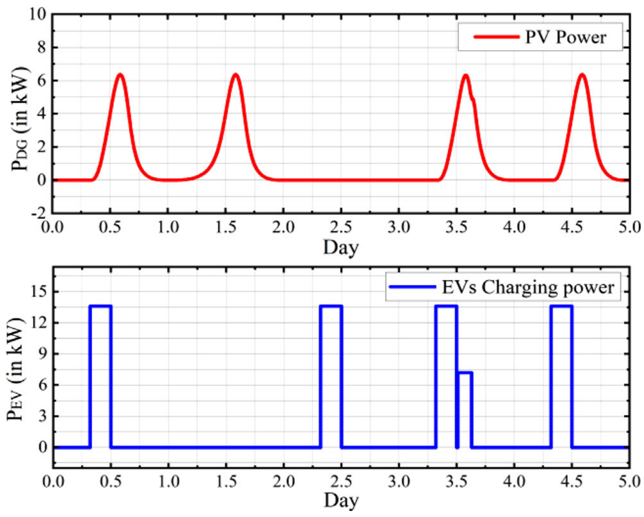

FIGURE 6 Input data of P_{DG} and P_{EV} (EVs charging demand).

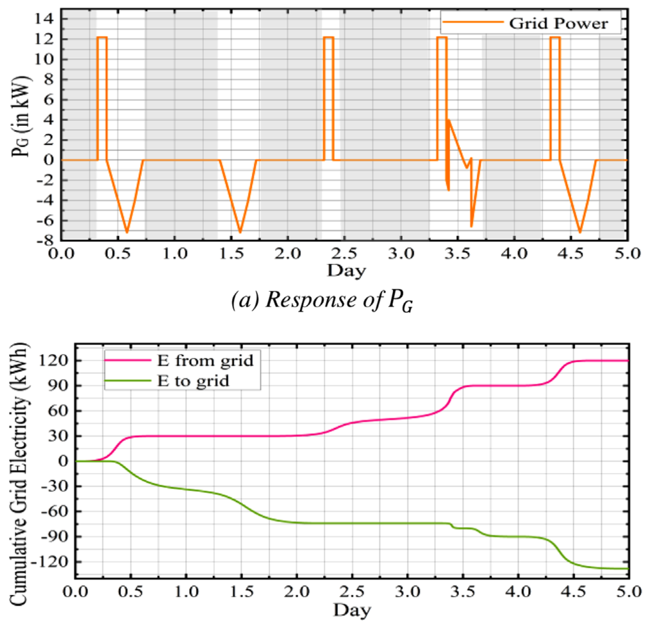

(b) Response of cumulative grid electricity

FIGURE 7 DG-powered EVCS without BSS. DG, distribution generation; EVCS, electric vehicle charging stations. (a) Response of P_G. (b) Response of cumulative grid electricity.

BSS is computed by DG electricity and EV load prediction. Here, the EVs charging mainly occurs during off-peak hours (from midnight till morning at 8 am). For the calculation of P_{EV}, the recharge energy is divided by the vehicle charging time. In both cases, the response of P_G and the aggregate of power (exchange between the EVCS and the grid) is designed for estimating the adverse impact of EVCS on the distribution grid.

To determine the charging pattern of the proposed site, a linearized fit model of the historical 3 months' data set is utilized from the previous EV charging load data set for a similar day of an individual week [52]. An online DERs estimation dataset is used to predict the average amount of existing solar electricity generation based on the amount of cloud cover.

Figure 7 indicates the increasing or growing by accumulation or successive additions of electricity consumption from the distributed grid and energy feeding into the distributed grid for the total period. From Figure 7 the measured P_G and cumulative grid electricity response for DGs-powered EVs charging stations without BSS is presented in Figure 7a. Here, the P_G response signifies the off-peak hours during the summer season for shaded areas scenarios. However, the power exchange between the distribution grid and EVCS is reduced by a factor of two as referred to in Figure 7b. It is a case of DG-powered EVCS without BSS, the positive amplitude (purple colour) indicates the energy consumption from the grid and the negative dip (green colour) indicates the energy fed into the grid. The negative value depicts the power supply into the grid, while the positive value depicts the power supply from the grid. In most cases in residential places, the charging of EVs operates in the early morning or night but more solar PV generation is available in the afternoon session [53]. So, solar-powered EVs charging may not be efficiently utilized in a residential place. Thus, this issue can be overcome by the consideration of a solar-powered charging system in the parking lot.

4.2 | Scenario 2: DG-powered EVCS with buffer BSS

Further, the typical scenario 2 of a DG-based EVs charging station with a buffer BSS is simulated in Figure 8. Instantaneously recharge the battery SoC up to 0.8 just after all possible charging events within 2 to 2.5 h. The recharging of BSS occurs during partial peak duration. In the case of SA operation mode (PV-powered EVCS without BSS), the incremented power requirement (which is fed from the grid) will be reduced. This simulation considers the Indian average power transmission and distribution losses of 17% to 20% [54]. Hence, the proposed PV-powered EVCS with a buffer BSS can reduce the transmission and distribution losses in a significant manner. In this scenario, the PV-powered EVCS is simulated for optimal SoC of BSS using similar inputs as referred from Figure 6. Figure 8 demonstrates the outcome of DG-powered EVs charging stations without BSS. The simulations of proposed EVs charging are performed under different cases.

In this scenario, the simulation result shows the PV-based EV charging for the proposed workplace (which includes an isolated PV plant system). Since the EVs charging happens in the morning session, so the solar-based DG power may not be directly utilized for EVCS. The P_G and the response of cumulative grid electricity has been plotted in Figure 8a as well as in Figure 8b, respectively. Here, the negative value of response shows the power supply into the distribution grid, as the positive value indicates the power supply from the distribution grid. Similarly, the power exchange between the distribution grid and EVCS is reduced by a factor of two as referred to in Figure 8b. The response of Figure 8b is represented by the green curve which

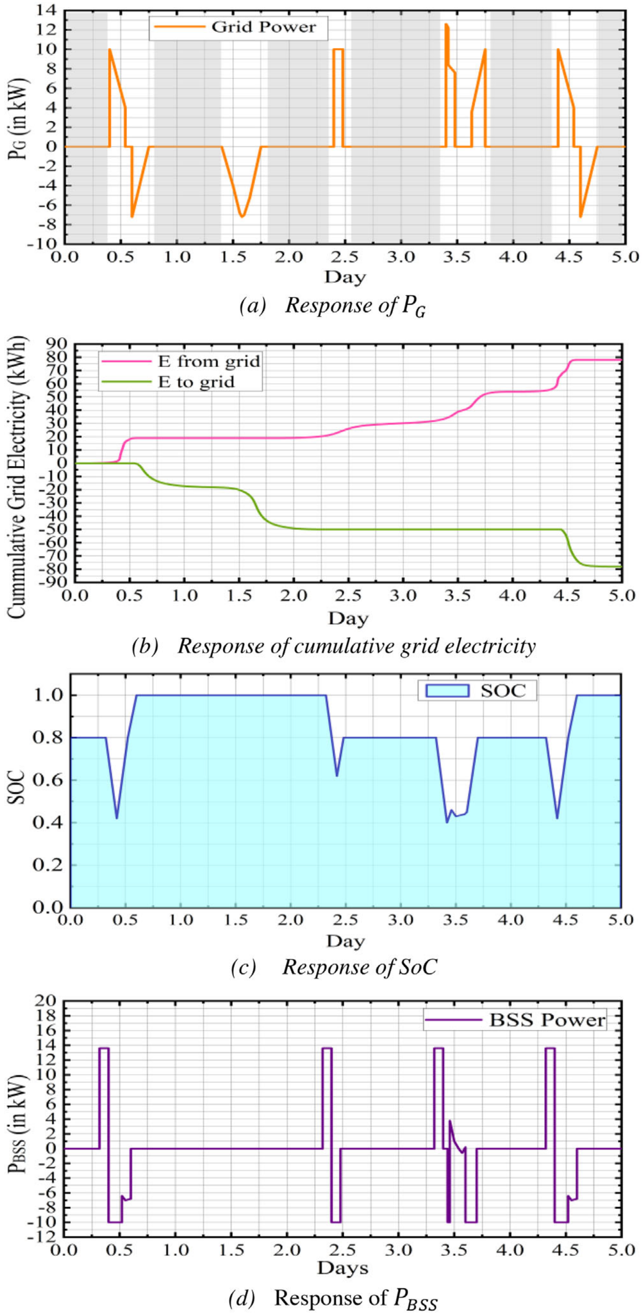

(a) Response of P_G

(b) Response of cumulative grid electricity

(c) Response of SoC

(d) Response of P_{BSS}

FIGURE 8 Characteristics of EVs charging station with buffer BSS (recharged after all charging events). (a) Response of P_G. (b) Response of cumulative grid electricity. (c) Response of SoC. (d) Response of P_{BSS}.

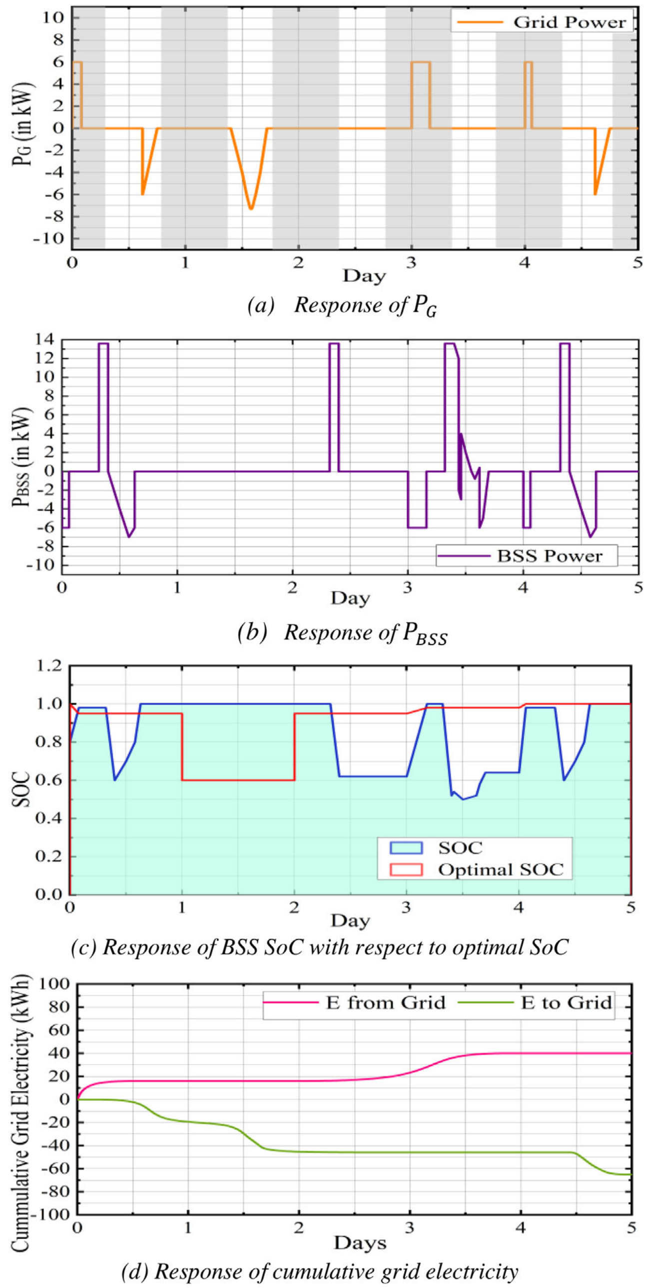

(a) Response of P_G

(b) Response of P_{BSS}

(c) Response of BSS SoC with respect to optimal SoC

(d) Response of cumulative grid electricity

FIGURE 9 DG-powered EVs charging with intelligent energy management. (a) Response of P_G. (b) Response of P_{BSS}. (c) Response of BSS SoC with respect to optimal SoC. (d) Response of cumulative grid electricity.

signifies the cumulative grid electricity power fed from the distribution grid. And the purple curve depicts the cumulative grid electricity supply into the distribution grid. In Figure 8c, an initial 0.8 SoC and a charging power of 10 kW are employed in the simulation. In Figure 8d, the purple line signifies the power flow variation of BSS based on the dis(charging).

The P_G is plotted in Figure 9a and analysed the P_{BSS} response in Figure 9b. In Figure 9c, the red line signifies the optimal SoC target, which is upgraded at midnight based on the input dataset. And the cumulative grid electricity response is referred to in Figure 9d. In the case of EVs charging demand exceeds the generated capacity of PV system, so the distribution grid provided the surplus electricity to fulfill the EVs charging demand; thus, power flow operation remains maintained without any interruption. So, it is concluded that the spikes of peak EVs load demand power on the distribution grid are significantly reduced. The purple curve in Figure 9d is the case of DG-powered EVs charging with intelligent energy management which provides more electricity to the grid. Practically, the supervised independent system operator will compare the measured SoC of BSS with the nominal SoC level to choose whether recharging of the BSS is required or not, especially during

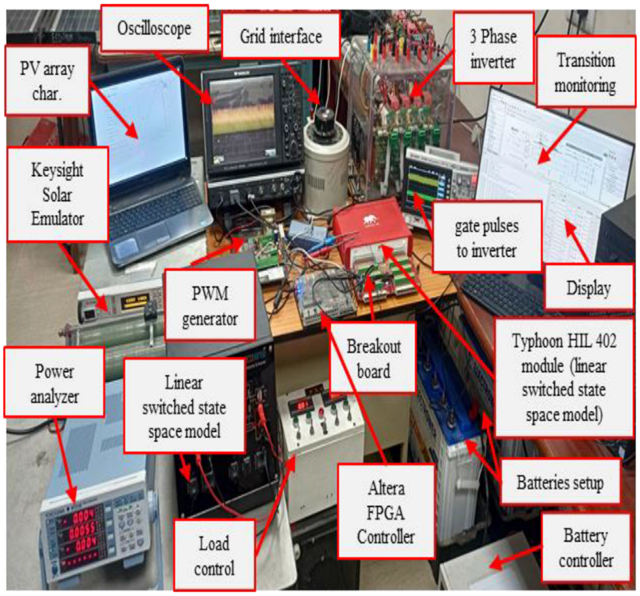

FIGURE 10 Experimental verification of intelligent Energy Management Scheme (EMS) operation.

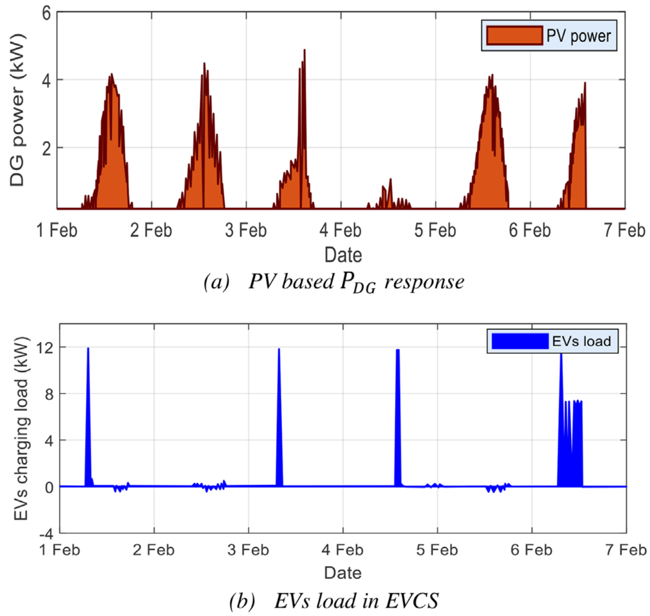

FIGURE 11 Measured P_{DG} and P_{EVCS} (charging EVs). (a) PV-based P_{DG} response. (b) EVs load in EVCS.

the off-peak period. Here, the P_{Peak} demand is decreased by a factor of two, similar to Figure 7b. The BSS recharges the demanded power by shifting the on-peak duration to the off-peak duration. As a result, a coordinated controller enhances the energy management approach. Since, all distribution companies (DISCOs) should be an employee of transition control in desired isolated/GC operational mode. Here, the IEMS offered flexibility for the EVCS fleet aggregator with optimal SoC based on forecasted local PV generation activities and further it will be beneficial for the planning of EVs power consumption on daily basis by local GENCOs. Therefore, the proposed intelligent EMS will be helpful in less power utilization during peak hour's duration. The proposed system further compares the actual SoC of BSS with the desired SoC in order to choose that recharging of BSS is required during the off-peak hours.

5 | EXPERIMENTAL VALIDATION

The developed coordinated control is experimentally validated through the hardware setup shown in Figure 10. The PV subsystem is emulated with a Keysight PV array simulator which is connected at the DC link of the Semikron 3ϕ four-leg DC to DC and further DC to AC converter configuration. The converter integrates the lead-acid batteries as vehicle charging loads and BSS in a coordinated system. A general linear load is connected in the system and all of this configuration is connected to the grid through a point of common coupling. The control is realized with the Typhoon HIL real-time simulator, and the coordinated control is implemented by configuring the HIL software and the Altera cyclone-IV field-programmable gate array (FPGA). This controller is motivated for accomplishing three main functions, that is, optimal monitoring, control strategy, and optimization of energy storage. The switching pulses are generated from the current controller developed based on the proportional resonant controller in the typhoon-HIL simulation. This controller operates according to the voltage levels and current limits in the system and generates the switching pulses which can be extracted as digital outputs from typhoon HIL 402. Further, the obtained digital signals are boosted to operate the VSC. The experimental setup is displaying the switching pulses are fed to the inverter. Further, the Hardware-HIL integration configuration with simulated components provides the pulses to the Semikron inverter. To accommodate the impact of extreme conditions where the forecasting algorithms may result in a mismatch of the information, the ANFIS controller framework can be accommodated with memory and replay buffer storage. These aspects provide an opportunity for the real-time monitoring system to store the scenarios related to the worst scenarios, which can be used further while implementing proposed algorithms for power flow management. The experimental analysis provides a real-time verification for the operation of the designed control approach under uncertainties in PV power generation and dynamic load.

The ANFIS controller model examined in this section is utilized to forecast and control the power flow sharing between the DG system and BSS which is based on the historical EV charging load data set [55, 56]. The EVCS was controlled for 7 days with the BSS being recharged throughout the off-peak duration (if the desired SoC level reaches to a lower value). Figure 11a demonstrates the measured P_{DG} based on PV-based generation. The overall EVCS load corresponding to the P_{DG} on daily basis is referred in Figure 11b.

Figure 12a shows the P_G characteristic associated with EVCS without buffer BSS. In Figure 12b, the P_G is evaluated for charging the EVCS with a buffer BSS based on the measured value of P_{DG} and EVs load in order to do comparative analysis

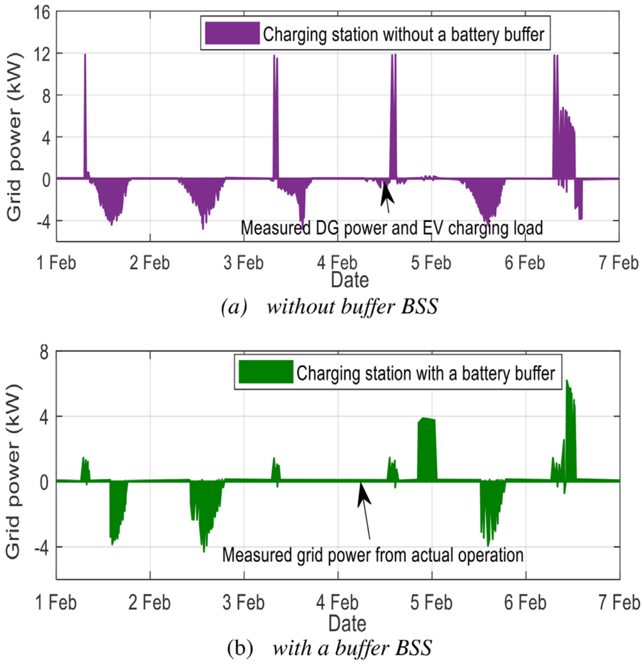

FIGURE 12 Characteristics of P_G for the EVs charging station. (a) Without buffer BSS. (b) With a buffer BSS.

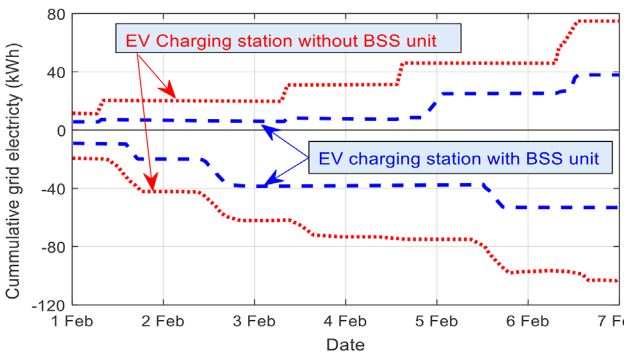

FIGURE 13 Response of P_{BSS} and cumulative grid electricity.

without a buffer BSS. Thus, the overall impact of EVCSs on the P_G utilization with/without BSS for the optimal value of BSS SoC is clearly evident from Figure 12. From the simulation results, solar-based DG power cannot be directly utilized for EVCS with the buffer BSS, which is accountable for reducing the power during peak hours.

Figure 13 illustrates the cumulative distribution of grid electricity. In order to show the comparison of EVCS with/without the buffer BSS, the proposed system includes a buffer BSS for some instant of time. Hence, the electricity transfer between the EVCS and the grid was decreased by a factor of two. Here, the BSS is operated with an EVCS continuously for a period of time with optimizing the BSS in order to collect the forecasted DG data sets based on the EVCS load. As a result, Figure 14 depicts the forecasted PV-based DG power and the actual generated PV-powered electricity using the proposed IEMS. Figure 13 shows the response of cumulative grid electricity correspond-

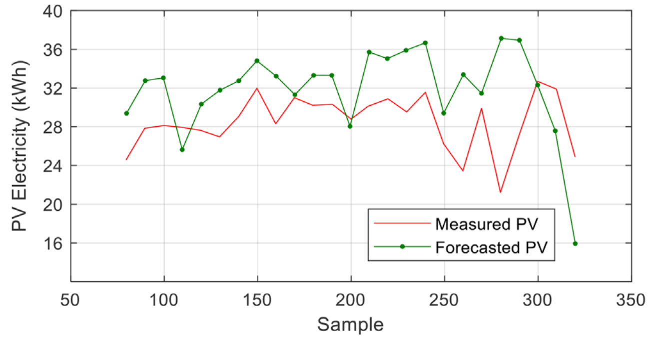

FIGURE 14 Prediction of DGs-based PV electricity generation for individual instant.

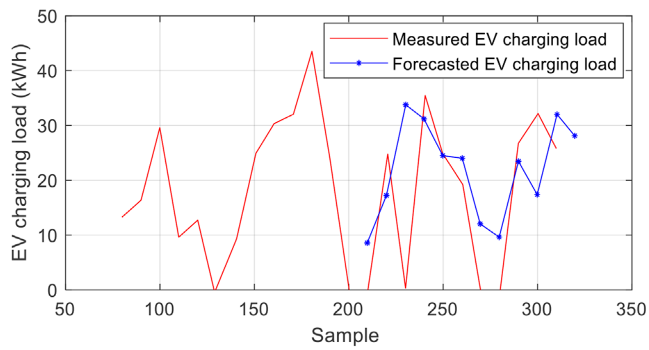

FIGURE 15 EVCS load forecasting for individual instant.

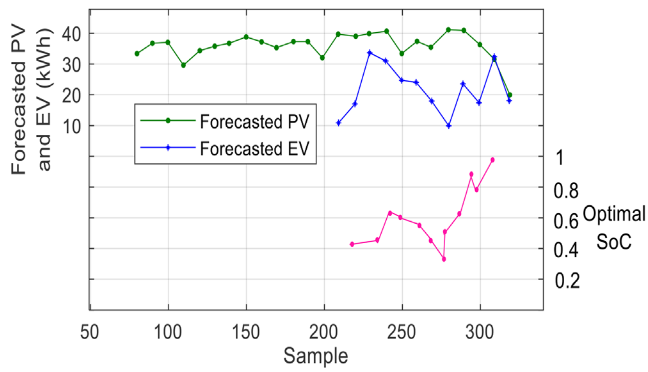

FIGURE 16 Targeted SoC of optimal BSS with respect to forecasted P_{DG} and P_{EV}.

ing to the operation of case (a) EV charging without a BSS unit and case (b) EV charging with BSS unit, respectively. The total electricity feed from the local grid during simulation period for case (a) is 76 kWh and for case (b) is 36 kWh. Similarly, the total electricity feed to the local grid during simulation period for case (a) is 103 kWh and for case (b) is 56 kWh. Thus, it can be concluded from Figure 13 that with respect to case (a) (i.e., 103 + 76 = 179 kWh) in case (b) (i.e., 36 + 56 = 92 kWh) the EVCS peak energy demand and electricity exchange with the local grid is dropped by a factor of 1.94 (which is approximately equal to a factor of 2). Thus, it directly decreases the burden of EVCS load on the local grid. In Figures 14–16, sample data stand for validation of forecasted data sets on an individual day.

TABLE 5 Comparative analysis between conventional and proposed coordinated intelligent control scheme

Parameter	Conventional EVCS control strategies [26, 27]	Without buffer BSS	With fixed buffer BSS [57]	Proposed coordinated control scheme
Grid impact	Higher	Higher	Moderate	Lower
IEMS	No	No	Yes	Yes
PV and EVs load prediction	No	No	No	Yes

In most cases, the PV electricity forecast is 15% to 18% greater than the actual generated PV power, which is mainly because of the PV panels' actual conversion efficiency not being as high as reported in their datasheet or by the variation in weather conditions. Due to inaccurate cloud cover information, the PV electricity forecast on several cloudy days has been much lower than the actual electricity generated. The ANFIS controller controls the active power flow among the different power system components and optimizes the BSS as per the forecasted PV generation and the EVCS load demand.

Figure 15 illustrates the measured charging load of EVs and the prediction for the EVs charging load on daily basis. The forecasted EVs charging load nearly displays the actual EV charging load variations. The desired SoC of BSS was optimized as per the forecasted PV-based electricity and forecasted EVCS load. If the SoC is lower than the optimal SoC level, then the BSS is recharged during off-peak periods. The PV electricity forecasts, EVCS load forecasts, and the desired SoC of BSS can be simulated on a daily or weekly basis. In Figure 15, EV charging load demand started from 210 samples to 327 samples is represented by a blue line. Correspondingly, the optimal SoC is calculated, which is represented for individual BSS on a scale of 0 to 1 as shown in Figure 16.

Figure 16 assesses the measured SoC compared to a fixed target SoC. It shows the forecasted PV and EVs load with optimal SoC for Sunday. Here, the optimal SoC represents the BSS individually on a scale of 0 to 1 in Figure 16. The forecasted EVs charging load almost matched the actual loads. Since the present simulated charging station has only one charger port, the result of the EVs load demand prediction will be affected by uncertainty and abnormalities/contingency.

Figure 17 illustrates the results of continuous operation based on a different sample of any individual day. The EV charging system was operated for 2800 sample, and the EVs were charged from the distribution grid. In the 1700th sample the ANFIS controller took over coordinate control of the EVCS and in the 1100th sample, the optimal utilization feature of the BSS was enabled. The EVCS demand load, P_{DG}, and P_G are plotted in Figure 17. The designed forecasted model results are indicating that intelligent EMS control approximately eliminates the peak electricity demands of the EVCS load demand from the distribution grid. As a result, the peak demand power has been reduced by a factor of two. In Table 5, the results of the developed coordinated control approach are compared with the conventional charging strategies available in the existing literature.

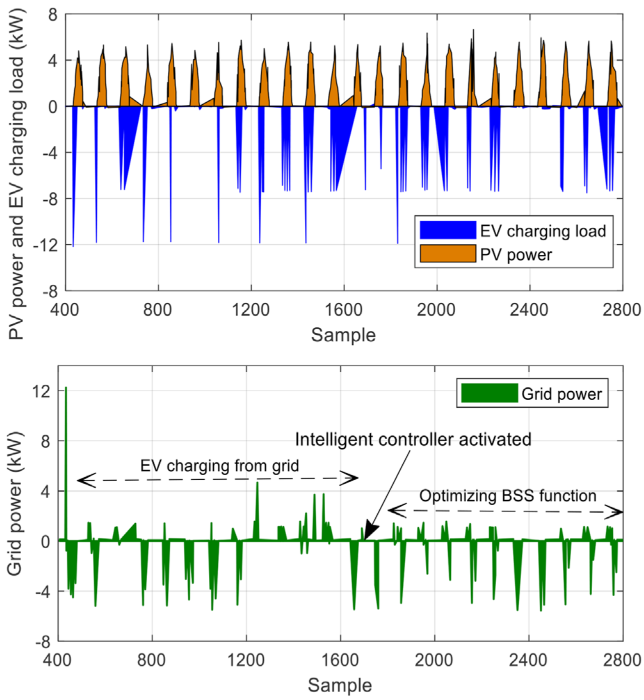

FIGURE 17 Measured EV charging load, P_{DG} and P_G.

From the comparative result of Table 5, it is identified that the intelligent controller along with the optimized battery SoC target has almost eliminated the peak electricity demand of the EVCS on the distribution grid. It is concluded that in our IEMS a large capacity battery will reduce the impact on the grid but increase the overall cost of the system. Hence, this research developed a cost-effective approach to effectively utilize the battery power and this achieves a more efficient operation. The EVs charging station with a BSS unit has a significant reduction in peak power demand when compared with the charging station without a buffer BSS unit. The transition strategy has advantages with disconnecting the DG system from the main distributed grid under off peak or grid failure conditions and reconnected without the battery storage unit.

6 | CONCLUSIONS

In this paper, an IEMS is developed to reduce the grid peak load and maximize the utilization of forecasted PV power for EVs charging load. Based on the actual EVCS load data set and meteorological data, the coordinated control strategy proves that the proposed IEMS scheme is feasible to optimize the BSS. Optimal battery SoC targets were determined by forecasting PV generation and estimating the EVs charging loads. Further, an ANFIS-based intelligent controller was developed and integrated into level 2 charging stations to execute the coordinated control strategy in order to utilize the BSS (with or without buffer storage), forecast PV-based DG power, and estimate EVs charging loads using HIL experimental setup. The proposed study demonstrated that EVs users routinely can use the intelligent controller integrated with the charging system at a time. Both simulation results and experimental results show that vehicle charging demands occur most frequently during the early morning period (when solar irradiance is not available), and hence the PV system is not able to supply the EVs charging demand. Therefore, the grid meets the EVCS demand at that time using IEMS. However, when the coordinated controller controls the BSS, then EVCS reduced its peak power demand and its energy exchange between PV generation, distribution grid, and EV battery storage resulting in the reduction of peak power demand by a factor of two. As a result, it shifts the BSS charging power demand from the on-peak period to the off-peak period which will benefit the owner of the EV charging station in consuming less energy during peak usage hours.

Further, the control capabilities of the developed IEMS can be improved by designing an agent-based online control scheme. This can be motivated by reducing the peak EVs extreme/ultra-fast charging demand under sudden disturbances during peak load and optimize the BSS in a hybrid multigrid system. Also, the data related to preferred EV charging rate and time of stay at EVCS can be considered to modify the control approach. Moreover, V2G ancillary services can be integrated with the proposed algorithm. Hence, the aspect of considering V2G and other ancillary services in the grid as an addon for developing a power flow management approach can be potential future work. Economical constraints can be considered in IEMS as the potential future aspects of the research.

AUTHOR CONTRIBUTIONS

Mohammad Amir: Conceptualization, Data curation, Investigation, Methodology, Software, Validation, Writing—original draft; Zaheeruddin: Data curation, Investigation, Supervision, Visualization, Writing—review & editing; Ahteshamul Haque: Conceptualization, Data curation, Methodology, Resources, Supervision, Writing—review & editing; Farhad Ilahi Bakhsh: Data curation, Formal analysis, Supervision, Validation, Writing—review & editing; V. S. Bharath Kurukuru: Data curation, Investigation, Visualization, Writing—review & editing; Mostafa Sedighizadeh: Formal analysis, Visualization, Validation, Writing—review & editing.

ACKNOWLEDGEMENTS

The work done in this paper is by using instrument Hardware-In-the-Loop (HIL) Typhoon real time simulator, purchased from DST-PURSE scheme at Central Instrumentation Facility (CIF), S. Ramanujan Block, Jamia Millia Islamia (Central University), New Delhi, India.

CONFLICT OF INTEREST STATEMENT

The author(s) declared no potential conflicts of interest with respect to the research, authorship, and/or publication of this article.

FUNDING INFORMATION

This research received no specific grant from any funding agency in the public, commercial, or not for profit sectors.

DATA AVAILABILITY STATEMENT

There does not contain any third-party data. The original contributions of study are included in the article.

ORCID

Mohammad Amir https://orcid.org/0000-0003-3432-4217
Farhad Ilahi Bakhsh https://orcid.org/0000-0001-6452-512X
Mostafa Sedighizadeh https://orcid.org/0000-0003-3160-5435

REFERENCES

1. Impram, S., Varbak Nese, S., Oral, B.: Challenges of renewable energy penetration on power system flexibility: A survey. Energy Strateg. Rev. 31, 100539 (2020)
2. Nour, M., Chaves-Ávila, J.P., Magdy, G., Sánchez-Miralles, Á.: Review of positive and negative impacts of electric vehicles charging on electric power systems. Energies 13, 4675 (2020)
3. Ahmad, F., Khalid, M., Panigrahi, B.K.: An enhanced approach to optimally place the solar powered electric vehicle charging station in distribution network. J. Energy Storage 42, 103090 (2021)
4. Khan, S., Ahmad, A., Ahmad, F., Shafaati Shemami, M., Saad Alam, M., Khateeb, S.: A comprehensive review on solar powered electric vehicle charging system. Smart Sci. 6(1), 54–79 (2018)
5. shafiei, M., Ghasemi-Marzbali, A.: Fast-charging station for electric vehicles, challenges and issues: A comprehensive review. J. Energy Storage 49, 104136 (2022)
6. Danese, A., Torsæter, B.N., Sumper, A., Garau, M.: Planning of high-power charging stations for electric vehicles: A review. Appl. Sci. 12(7), 3214 (2022)
7. Farhadi, P., Moghaddas Tafreshi, S.M.: Charging stations for electric vehicles: A comprehensive review on planning, operation, configurations, codes and standards, challenges and future research directions. Smart Sci. 1–33 (2021)
8. Verma, A., Singh, B.: Multimode operation of solar PV array, grid, battery and diesel generator set based EV charging station. IEEE Trans. Ind. Appl. 56(5), 5330–5339 (2020)
9. Huang, N., He, Q., Qi, J., et al.: Multinodes interval electric vehicle day-ahead charging load forecasting based on joint adversarial generation. Int. J. Electr. Power Energy Syst. 143, 108404 (2022)
10. Amir, M., Zaheeruddin, Haque, A.: Integration of EVs aggregator with microgrid and impact of V2G power on peak regulation. In: 2021 IEEE 4th International Conference on Computing, Power and Communication Technologies (GUCON). IEEE, pp. 1–6 (2021)
11. Khan, M.A., Haque, A., Kurukuru, V.S.B.: Intelligent transition control approach for different operating modes of photovoltaic inverter. In: 2021 IEEE 12th Energy Conversion Congress & Exposition - Asia (ECCE-Asia). IEEE, pp. 1879–1884 (2021)
12. Ameli, A., Farrokhifard, M.-R., Davari-nejad, E., Oraee, H., Haghifam, M.-R.: Profit-based DG planning considering environmental and

operational issues: A multiobjective approach. IEEE Syst. J. 11(4), 1959–1970 (2017)
13. Huang, L., Xin, H., Li, Z., et al.: Grid-synchronization stability analysis and loop shaping for PLL-based power converters with different reactive power control. IEEE Trans. Smart Grid 11(1), 501–516 (2020)
14. Zaheeruddin, Singh, K., Amir, M.: Intelligent fuzzy TIDF-II controller for load frequency control in hybrid energy system. IETE Tech. Rev. 1–17 (2021)
15. Islam, M.A., Singh, J.G., Jahan, I., et al.: Modeling and performance evaluation of ANFIS controller-based bidirectional power management scheme in plug-in electric vehicles integrated with electric grid. IEEE Access 9, 166762–166780 (2021)
16. Clairand, J.-M., Álvarez-Bel, C., Rodríguez-García, J., Escrivá-Escrivá, G.: Impact of electric vehicle charging strategy on the long-term planning of an isolated microgrid. Energies 13(13), 3455 (2020)
17. Feng, J., Yang, J., Li, Y., et al.: Load forecasting of electric vehicle charging station based on grey theory and neural network. Energy Rep. 7, 487–492 (2021)
18. Khan, M.A., Haque, A., Blaabjerg, F., Kurukuru, V.S.B., Wang, H.: Intelligent transition control between grid-connected and standalone modes of three-phase grid-integrated distributed generation systems. Energies 14(13), 3979 (2021)
19. Mateen, S.: Discrete stochastic control for energy management with photovoltaic electric vehicle charging station. CPSS Trans. Power Electron. Appl. 7(2), 216–225 (2022)
20. van der Meer, D., Chandra Mouli, G.R., Morales-Espana Mouli, G., Elizondo, L.R., Bauer, P.: Energy management system with PV power forecast to optimally charge EVs at the workplace. IEEE Trans. Ind. Inform. 14(1), 311–320 (2018)
21. Dukpa, A., Butrylo, B.: MILP-based profit maximization of electric vehicle charging station based on solar and EV arrival forecasts. Energies 15(15), 5760 (2022)
22. Sanchez-Martin, P., Lumbreras, S., Alberdi-Alen, A.: Stochastic programming applied to EV charging points for energy and reserve service markets. IEEE Trans. Power Syst. 31(1), 198–205 (2016)
23. Van Kriekinge, G., De Cauwer, C., Sapountzoglou, N., Coosemans, T., Messagie, M.: Day-ahead forecast of electric vehicle charging demand with deep neural networks. World Electr. Veh. J. 12(4), 178 (2021)
24. Ying, X.: An overview of overfitting and its solutions. J. Phys. Conf. Ser. 1168, 022022 (2019)
25. Amir, M., Zaheeruddin, Haque, A.: Optimal scheduling of charging/discharging power and EVs pattern using stochastic techniques in V2G system. In: 2021 IEEE Transportation Electrification Conference (ITEC-India). IEEE, pp. 1–6 (2021)
26. Chandra Mouli, G.R., Bauer, P., Zeman, M.: System design for a solar powered electric vehicle charging station for workplaces. Appl. Energy 168, 434–443 (2016)
27. Zhang, W., Zhang, D., Mu, B., et al.: Decentralized electric vehicle charging strategies for reduced load variation and guaranteed charge completion in regional distribution grids. Energies 10(2), 147 (2017)
28. S, S.M., Titus, F., Thanikanti, S.B., M, S.S., Deb, S., Kumar, N.M.: Charge scheduling optimization of plug-in electric vehicle in a PV powered grid-connected charging station based on day-ahead solar energy forecasting in Australia. Sustainability 14(6), 3498 (2022)
29. Chis, V., Barbulescu, C., Kilyeni, S., Dzitac, S.: ANN based short-term load curve forecasting. Int. J. Comput. Commun. Control 13, 938–955 (2018)
30. Rao, S.N.V.B., Yellapragada, V.P.K., Padma, K., et al.: Day-ahead load demand forecasting in urban community cluster microgrids using machine learning methods. Energies 15(17), 6124 (2022)
31. Radosevic, N., Liu, G.-J., Tapper, N., Zhu, X., Sun, Q.: (Chayn): Solar energy modeling and mapping for the sustainable campus at Monash University. Front. Sustain. Cities 3, 745197 (2022)
32. Jayaswal, K., Sharma, G.S., Bhaskar, M.S., Almakhles, D.J., Subramaniam, U., Palwalia, D.K.: Global solar insolation estimation and investigation: A case study of various nations and cities. IEEE Access 9, 88069–88084 (2021)
33. Open Weather: Solar Radiation API. https://openweathermap.org/api/solar-radiation
34. Kumar, D.: Satellite-based solar energy potential analysis for southern states of India. Energy Rep. 6, 1487–1500 (2020)
35. NREL: Solar, Load, and Tariff Resource Data. https://www.nrel.gov/grid/solar-resource/renewable-resource-data.html
36. Jayachandran, M., Reddy, C.R., Padmanaban, S., Milyani, A.H.: Operational planning steps in smart electric power delivery system. Sci. Rep. 11(1), 17250 (2021)
37. Xiao, Z., Zhou, Y., Cao, J., Xu, R.: A medium- and long-term orderly charging load planning method for electric vehicles in residential areas. World Electr. Veh. J. 12(4), 216 (2021)
38. Cao, Y., Wang, H., Li, D., Zhang, G.: Smart online charging algorithm for electric vehicles via customized actor-critic learning. IEEE Internet Things J. 1–11 (2021)
39. Boulmrharj, S., Ouladsine, R., NaitMalek, Y., et al.: Online battery state-of-charge estimation methods in micro-grid systems. J. Energy Storage 30, 101518 (2020)
40. Simolin, T., Rautiainen, A., Koskela, J., Järventausta, P.: Control of EV charging and BESS to reduce peak powers in domestic real estate. Int. Rev. Electr. Eng. 14(1), 1 (2019)
41. Mohammad, A., Zamora, R., Lie, T.T.: Transactive energy management of PV-based EV integrated parking lots. IEEE Syst. J. 15(4), 5674–5682 (2021)
42. Chang, K.-C., Hagumimana, N., Zheng, J., et al.: Standalone and minigrid-connected solar energy systems for rural application in Rwanda: An in situ study. Int. J. Photoenergy 2021, 1–22 (2021)
43. Ferraro, M., Brunaccini, G., Sergi, F., Aloisio, D., Randazzo, N., Antonucci, V.: From uninterruptible power supply to resilient smart micro grid: The case of a battery storage at telecommunication station. J. Energy Storage 28, 101207 (2020)
44. Kaur, S., Kaur, T., Khanna, R.: ANFIS based smart control of electric vehicles integrated with solar powered hybrid AC-DC microgrid. Electr. Power Components Syst. 48(12–13), 1282–1295 (2020)
45. Urrea, C., Morales, C.: Enhancing Modbus-RTU communications for smart metering in building energy management systems. Secur. Commun. Netw. 2019, 1–8 (2019)
46. Fu, X., Li, S.: Control of single-phase grid-connected converters with LCL filters using recurrent neural network and conventional control methods. IEEE Trans. Power Electron. 31(7), 5354–5364 (2016)
47. Bawazir, R.O., Cetin, N.S.: Comprehensive overview of optimizing PV-DG allocation in power system and solar energy resource potential assessments. Energy Rep. 6, 173–208 (2020)
48. Amir, M., Haque, A., Kurukuru, V.S.B., Bakhsh, F., Ahmad, A.: Agent based online learning approach for power flow control of electric vehicle fast charging station integrated with smart microgrid. IET Renew. Power Gener. n/a-n/a (2022)
49. Ayoub, S., Haque, A., Amir, M., Kurukuru, V.S.B.: Intelligent islanding classification with optimal k-nearest neighbors technique for single phase grid integrated PV system. In: 2022 IEEE 3rd Global Conference for Advancement in Technology (GCAT). IEEE, pp. 1–6 (2022)
50. Agin, F., Khosravanian, R., Karimifard, M., Jahanshahi, A.: Application of adaptive neuro-fuzzy inference system and data mining approach to predict lost circulation using DOE technique (case study: Maroon oilfield). Petroleum 6(4), 423–437 (2020)
51. Minaev, O.M., Vakhazhi, K.-M.M., Uspanova, A.S.: Algorithm for selecting input variables for solving the problem of forecasting the set of entrants using the ANFIS neuro-fuzzy system. In: AIP Conference Proceedings, vol. 2442, pp. 040005 (2021)
52. ENTSO-E: Monthly Hourly Load Values.
53. Fretzen, U., Ansarin, M., Brandt, T.: Temporal city-scale matching of solar photovoltaic generation and electric vehicle charging. Appl. Energy 282, 116160 (2021)
54. The Economics Times: Economic Survey flags high T&D losses in Indian Power Sector (2022)

55. Selvaraju, R.K., Somaskandan, G.: ACS algorithm tuned ANFIS-based controller for LFC in deregulated environment. J. Appl. Res. Technol. 15(2), 152–166 (2017)
56. Amir, M., Zaheeruddin, Haque, A.: Intelligent based hybrid renewable energy resources forecasting and real time power demand management system for resilient energy systems. Sci. Prog. 105(4), 003685042211321 (2022)
57. Korkas, C.D., Baldi, S., Yuan, S., Kosmatopoulos, E.B.: An adaptive learning-based approach for nearly optimal dynamic charging of electric vehicle fleets. IEEE Trans. Intell. Transp. Syst. 19(7), 2066–2075 (2018)

How to cite this article: Amir, M., Zaheeruddin, Haque, A., Bakhsh, F.I., Kurukuru, V.S.B., Sedighizadeh, M.: Intelligent energy management scheme-based coordinated control for reducing peak load in grid-connected photovoltaic-powered electric vehicle charging stations. IET Gener. Transm. Distrib. 1–18 (2023). https://doi.org/10.1049/gtd2.12772